RSC Advances

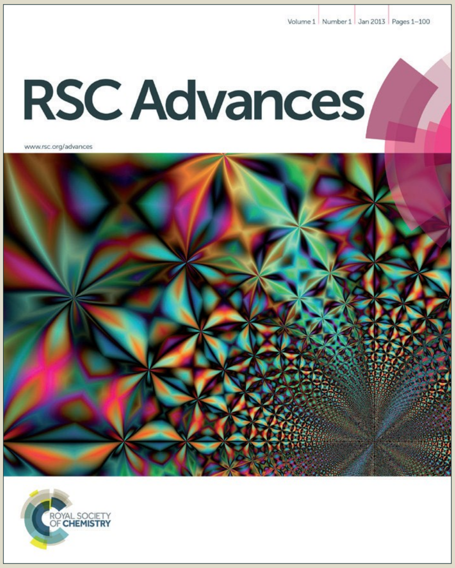

Volume 1 | Number 1 | Jan 2013 | Pages 1–100

RSC Advances

www.rsc.org/advances

ROYAL SOCIETY OF CHEMISTRY

ROYAL SOCIETY OF CHEMISTRY

www.rsc.org/advances

Journal Name

RSCPublishing

ARTICLE

In Situ Access to Fluorescent Dual-Component Polymers towards Optoelectronic Devices via Inhomogeneous Biphase Frontal Polymerization

Cite this: DOI: 10.1039/x0xx00000x

Received 00th January 2012,
Accepted 00th January 2012

DOI: 10.1039/x0xx00000x

www.rsc.org/

Qing Li, Wan-chao Zhang, Cai-Feng Wang, and Su Chen*

Herein, we report the in-situ synthesis of dual-component poly(AM-*co*-NVP) and poly(HEA-*co*-NVP) polymers (AM = Acrylamide, HEA = 2-hydroxyethyl acrylate, NVP = 1-vinyl-2-pyrrolidone) based on two incompatible phases via laser-ignited inhomogeneous biphase frontal polymerization (FP) within 10 min. Once initiated, the monomers converted to polymer spontaneously without the need of any external energy owing to the traits of exothermic polymerization, providing a facile, rapid and cost-effective approach. The dependence of the frontal velocities and temperatures on initiator concentration and the monomer weight ratio was systematically investigated. Moreover, an operable bilayer film with two fluorescent signals was obtained by simply introducing fluorescent carbon dots (CDs) and quantum dots (QDs). The as-prepared fluorescent bilayer film realized white light emission and could be conveniently applied onto a commercial UV light-emitting diode (LED) to generate white LEDs. We believe the methodology developed in this work may promote the development of various inhomogeneous multicomponent polymers and LED nanocomposite in a fast and efficient way.

1. Introduction

Frontal polymerization (FP)[1-5] is an exothermic polymerization coupled with thermal diffusion and Arrhenius kinetics, which is discovered by Chechilo et al. in 1972[1]. Compared to other widely used polymerization techniques, this polymerization model converts monomers into polymer by the propagation of a localized reaction zone through the whole system. Once ignited, no further energy is required in the coming reaction process. Because of the unique advantages of high reaction rates, convenient operation and less energy-consuming, FP has attracted extensive attention in the preparation of various polymers. Up to now, plenty of homogeneous polymers have been fabricated via FP, such as polyurethane materials[6,7], gradient materials[8,9], thermochromic composites[10], interpenetrating polymer networks (IPNs)[11,12] and especially functional hydrogels[13-21]. Besides, a large amount of work have been devoted to developing new frontal polymerization patterns based on three types of FP: thermal frontal polymerization (TFP)[22,23], photoinitiated frontal polymerization[24-27], and isothermal frontal polymerization[28]. Very recently, our group proposed plasma-ignited frontal polymerization[29,30], infrared laser-ignited frontal polymerization[31-34], magnetocaloric effect-induced frontal polymerization[35,36] and the latest anisotropic biphase frontal polymerization[37] in the preparation of hydrogels with versatile functions. Despite dramatic progress have been made in the synthesis of single component polymers, there are no reports on multicomponent polymers [38-42] via FP except one example for synthesis of the dual-component poly(TMPTA-*co*-HEA) and poly(HEA-*co*-NVP) polymers which used as fluorescent 2D codes for chemical recognition of organic amines[37].

Herein, taking advantage of the latest laser ignited biphase continuous frontal polymerization model, we realized the facile and controllable in-situ synthesis of dual-component poly(AM-*co*-NVP) and poly(HEA-*co*-NVP) continuous polymers for the first time within 10 min by combining two immiscible phases, the phase-1 (the monomers of AM and NVP dissolved in DMSO) and phase-2(the monomers of HEA and NVP dissolved in glycerol) (Scheme 1). By simply introducing fluorescent carbon dots (CDs) and quantum dots (QDs), a dual-component bilayer film with two fluorescent signals toward in-situ generation of white light-emitting fluorescent polymer nanocomposites with well combined properties was first prepared via frontal polymerization in horizontal direction, and meanwhile avoiding the emergence of photooxidation, photocorrosion, or luminescence diminishing in other methods. Moreover, the as-prepared fluorescent bilayer film was conveniently applied onto a commercial UV light-emitting diode (LED) to generate white LEDs, indicating potential applications in optoelectronic devices. This easy-to-perform polymerization pattern for the synthesis of fluorescent dual-component polymers developed here may provide an available and efficient avenue to in situ fabricate functional multicomponent polymers towards optoelectronic devices.

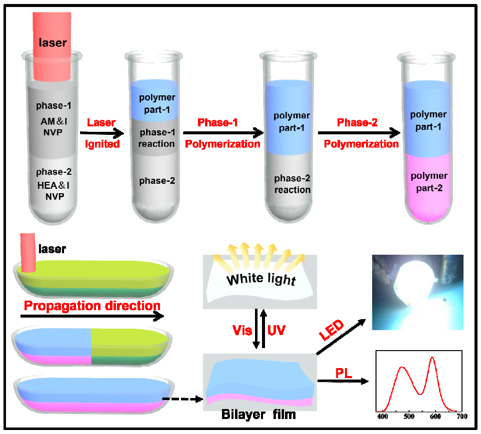

Scheme 1 Schematic illustration of the fabrication route to prepare dual-component poly(AM-*co*-NVP) and poly(HEA-*co*-NVP) polymers via inhomogeneous biphase FP.

2. Experiment

2.1 Materials

Acrylamide (AM), 2-hydroxyethyl acrylate (HEA), 1-vinyl-2-pyrrolidone (NVP), tellurium powder (Te), sodium borohydride (NaBH4), glycerol, dimethylsulfoxide (DMSO), N-acetyl-L-cysteine (NAC), cadmium chloride ($CdCl_2$), N,N′-methylenebisacrylamide (MBAA) were purchased from Aldrich. The redox couple, ammonium persulfate (APS)/N,N,N′,N′-tetramethylethylenediamine (TMEDA) was also obtained from Aldrich. All chemicals were commercially available with analytical grade and used as received.

2.2 Laser ignited inhomogeneous biphase FP of the dual-component polymers with poly(AM-*co*-NVP) and poly(HEA-*co*-NVP)

Two mixtures were prepared in independent beaks. First, an appropriate amount of APS (initiator) was dissolved in DMSO ultrasound, following by introducing AM, MBAA and NVP with vigorous stirring until complete dissolution. Then, the TMEDA was added into the homogeneous mixture solution (phase-1). A typical composition of phase-1 was AM/NVP = 8:2 wt/wt, DMSO = 50 wt%, MBAA = 0.3 wt%, APS = 0.2 wt%, [APS]/[TMEDA] = 1:4 mol/mol. For the preparation of phase-2, NVP, HEA, MBAA, glycerol and APS (initiator) were added into the second beaker to obtain a homogeneous mixture with vigorous stirring, followed by adding TMEDA. A typical composition was HEA/NVP = 8:2 wt/wt, glycerol = 50 wt%, MBAA = 0.25 wt%, APS = 0.2 wt%, [APS]/[TMEDA] = 1:4 mol/mol. The appropriate amounts of phase-2 and phase-1 solutions were sequentially converted to a glass test tube (10 mL; 15 mm diameter). An obvious phase interface could be clearly seen. Then, the filled tube was clamped into a holder and the upper side (phase-1) was heated by the laser until the hot propagating front commenced. The CO_2 laser which produces a beam of infrared light with the main wavelength bands centering around 10.6 μm was used to initiate the polymerization via heating ~10 s, where the radiating power density of the IR laser is 157 mW/cm^2. Finally, the continuous dual-component poly(AM-*co*-NVP) (denoted as polymer part-1) and poly(HEA-*co*-NVP) (denoted as polymer part-2) polymers were obtained with several minutes.

2.3 Velocity and temperature measurements

The front velocity was determined by calculating the slope of the line fit to the front position versus time. Constant front velocity in each phase implies the occurrence of pure free-radical FP. Temperature profiles were determined by measuring the temperature at a fixed point (which was selected in the phase-1 and the phase-2 mixture, respectively) as a function of time with Fluke Ti30 IR thermal imager. After reaction, the samples were cooled to room temperature and then removed from the tube for further investigation.

2.4 Material characterization

2.4.1 Fourier-transform infrared analysis

To investigate the chemical structure of as-prepared polymeric compounds, fourier transform infrared (FTIR) studies were carried out on a Nicolet-6700 spectrometer at room temperature. The samples were ground into a dry KBr disk. In all cases, 32 scans at a resolution of 4 cm^{-1} were used to record the spectra.

2.4.2 Thermogravimetric analysis

The thermal stability experiments of as-prepared samples were determined by using a thermogravimetric analysis (NETZSCH STA 449F3, Germany). The samples were combusted in nitrogen atmosphere with a heating rate of 10 °C/min from 0 to 800 °C.

2.4.3 SEM measurement

The surface microstructure of the samples obtained were investigated by SEM with a QUANTA 200 (Philips-FEI, Holland) at 20.0 kV. The sliced samples were immersed in excess deionized water at room temperature for a week. During this time, the water was changed daily to remove unreacted monomers and solvent. Afterward, the samples were dried in a vacuum baking oven at 60 °C until the weight of the samples was constant. The dried samples were then immersed in solution until they reached maximum swelling ratio. Subsequently, the samples were freeze-dried for 12 h. Dehydrated samples used for SEM measurement were cut to expose their inner structure.

2.4.4 Swelling Measurement

The swelling properties of the as-prepared hydrogels were performed by gravimetric analysis. The evacuated samples were weighed and immersed into a beaker with sufficient water and aqueous solutions of different pH values at room temperature. The samples were wiped off the solution on the surface with filter paper and weighed at regular time intervals. After weighing, the samples were returned to the swelling medium. The experiment was continued until the weight of the swollen samples was constant. The swelling ratio (SR, %) was calculated by the following equation:

$$SR = (W_i - W_0) / W_0 \times 100\% \quad (1)$$

Here, where W_i is the weight of swollen sample after a certain time and W_0 is the weight of the initial dried sample.

2.4.5 Fluorescence measurement

The N-acetyl-L-cysteine (NAC)-capped high-quality CdTe QDs and CDs were synthesized according to a modified literature procedure. The fluorescence properties of samples were measured with photoluminescence (PL) spectra. PL spectra were determined on a Varian Cary Eclipse fluorescence spectrophotometer at room temperature operating with a 380 nm laser beam as a light source with Xe-lamp as excited source, tube voltage was 600 V.

2.4.6 Fabrication of white light-emitting diode

For the fabrication of white LED, a UV-LED chip with the peak wavelength centered at 380 nm was attached on the bottom of the reflector cup by using conductive silver paste. The obtained fluorescent bilayer film was dried and ground into powders, which were then mixed with epoxy resin A and epoxy resin B (OE-6550A:OE-6550B) at the weight ratio of 1:1. The bubbles and solvent in the resin were removed in a vacuum chamber. Then, the mixture of silicone and nanophosphors was overcoated on the chip and cured at 150 °C for 60 min. After that, the reflector cup was capped with an optical lens, and the void was filled with transparent silicone. The ultimate LED was then further cured at 150 °C for 60 min. All the optical parameters were measured by a ZWL-600 Spectral Radiation Analyzer with an integrating sphere at room temperature.

3. Results and discuss

3.1 Laser ignited inhomogeneous biphase FP of the dual-component poly(AM-*co*-NVP) and poly(HEA-*co*-NVP) polymers

Several preliminary experiments were implemented to prepare dual-component poly(AM-*co*-NVP) and poly(HEA-*co*-NVP) polymers by inhomogeneous biphase FP with a stable front. "Fingering" phenomenon and Spontaneous polymerization (SP) are two main factors that destabilize the front in FP process. In order to avoid the interference of double-diffusive convection resulting in the "Fingering", Glycerol was chose as the medium of phase-2 solutions. Another essential factor for FP is the pot life, a period of time that the reagents can remain at ambient temperature before SP, was also evaluated by leaving the reactant mixture at room temperature and visually observing when they spontaneously polymerized. The results show that the reactant mixtures here are inert at the ambient temperature (20℃) for more than 6 hours but very reactive after being irradiated in several seconds. As shown in Scheme 1, there is a clear interface between the copolymer and the unreacted monomer. It is easy to distinguish the propagating front for the measurement of temperature and time.

A constant frontal velocity is the preliminary factor to verify the occurrence of pure FP without SP. The traveling front and reaction time are well fitted by two linear functions, indicating that a constant-velocity, self-sustaining front was obtained in each phase, as indicated in Figure 1. This is strong evidence that pure FP take place and the propagating velocities of phase-1 and phase-2 are 14.8 and 9.2 mm/min, respectively. Another key feature to confirm the occurrence of pure inhomogeneous biphase FP is given by the analysis of temperature profiles. As can be seen in Figure 2a-b, the horizontal part and maximum temperature (T_{max}) on both curves indicate no temperature variation that caused by the exothermicity of the SP reaction, which further confirms that pure FP occurs.

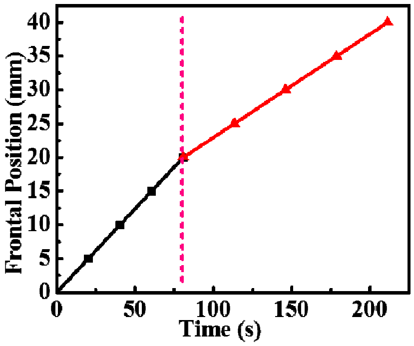

Fig. 1 Front position versus time for the dual-component poly(AM-*co*-NVP) and poly(HEA-*co*-NVP) polymers prepared by inhomogeneous biphase FP. Initial conditions: phase-1, AM/NVP = 8:2 (wt/wt), DMSO = 50 wt%, MBAA = 0.3 wt%, APS = 0.2 wt%, [APS]/[TMEDA] = 1:4 (mol/mol); phase-2, HEA/NVP = 8:2 wt/wt, glycerol = 50 wt%, MBAA = 0.25 wt%, APS = 0.2 wt%, [APS]/[TMEDA] = 1:4 (mol/mol).

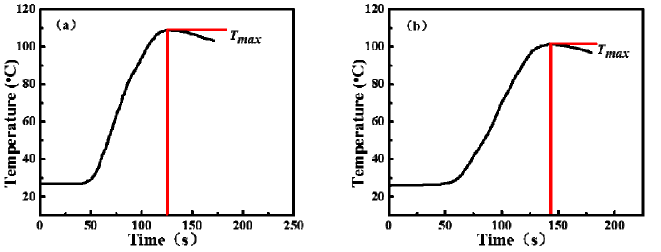

Fig. 2 Typical temperature profiles of (a) poly(AM-*co*-NVP) and (b) poly(HEA-*co*-NVP) polymers prepared by inhomogeneous biphase FP. Initial conditions: phase-1, AM/NVP = 8:2 (wt/wt), DMSO = 50 wt%, MBAA = 0.3 wt%, APS = 0.2 wt%, [APS]/[TMEDA] = 1:4 (mol/mol); phase-2, HEA/NVP = 8:2 wt/wt, glycerol = 50 wt%, MBAA = 0.25 wt%, APS = 0.2 wt%, [APS]/[TMEDA] = 1:4 (mol/mol).

3.2 Effects of the initiator concentration on inhomogeneous biphase FP

The initiator concentration is a significant factor in FP that as the initiator concentration exceeds to some degree, it becomes difficult to carry out FP while the reactive front of FP will be extinguished due to insufficient reaction-released heat with a relatively low initiator concentration. To optimize initiator concentration, several runs were performed at different APS concentration varying from 0.10 wt% to 0.30 wt% in each phase, whereas AM/NVP = 8:2 (wt/wt) in the phase-1 and HEA/NVP = 8:2 (wt/wt) in the phase-2. When the concentration of APS was higher than 0.30 wt%, many bubbles occurred and the as-prepared samples were not homogenous. On the contrary, the inhomogeneous biphase FP couldn't be carried out in the case of APS concentration less than 0.10 wt%. Therefore, all the dual-component poly(AM-*co*-NVP) and poly(HEA-*co*-NVP) polymers were prepared with APS concentration ranging from 0.10 wt% to 0.30 wt% in each phase. The front velocity and $T_{\max}$ of the dual-component poly(AM-*co*-NVP) and poly(HEA-*co*-NVP) polymers as a function of APS concentration is shown in Figure 3. As expected, both the front velocity and the $T_{\max}$ monotonically increased and followed a parallel trend with the increased amount of initiator. With the initiator concentration increasing from 0.10 to 0.30 wt%, $T_{\max}$ of phase-1 increased from 102 to 117 °C and $T_{\max}$ of phase-2 raised from 92 to 109 °C. It should be noted that all the inhomogeneous biphase FP runs were performed under nonadiabatic conditions, so the increased velocity reduced the time of heat loss, which led to the increase of $T_{\max}$.

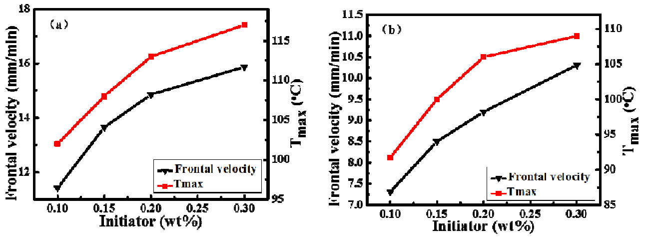

Fig. 3 Frontal velocity and $T_{\max}$ of the dual-component (a) poly(AM-*co*-NVP) and (b) poly(HEA-*co*-NVP) polymers prepared by inhomogeneous biphase FP versus the concentration of initiator. Initial conditions: phase-1, AM/NVP = 8:2 (wt/wt), DMSO = 50 wt%, MBAA = 0.3 wt%, [APS]/[TMEDA] = 1:4 (mol/mol); phase-2, HEA/NVP = 8:2 wt/wt, glycerol = 50 wt%, MBAA = 0.25 wt%, [APS]/[TMEDA] = 1:4 (mol/mol).

3.3 Effects of the monomer ratios on inhomogeneous biphase FP

The monomer weight ratio is also an important factor in FP and thus several runs of monomer mass ratios ranging from 8:2 to 5:5 (wt/wt) in each phase were performed to in-situ prepare dual-component poly(AM-*co*-NVP) and poly(HEA-*co*-NVP) polymers. The front velocity and $T_{\max}$ as a function of monomer mass ratios is shown in Figure 4. When the monomer weight ratios ranged from 8:2 to 5:5 (wt/wt), the phase-1 frontal velocities varied from 14.85 to 11.63 mm/min, and the corresponding $T_{\max}$ decreased from 113 to 95.8 °C, respectively, while the phase-2 frontal velocities varied from 9.2 to 7.69 mm/min, and the corresponding $T_{\max}$ decreased from 106 to 90.9 °C, respectively. This could be attributed to the lower reactivity of NVP toward radical polymerization that higher NVP concentration generates less reactive heat, thus leading to the decrease of front velocity.

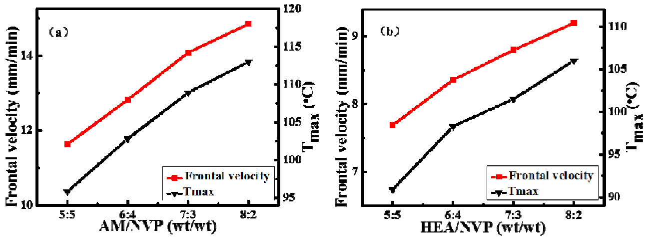

Fig. 4 Frontal velocity and $T_{\max}$ of the dual-component (a) poly(AM-*co*-NVP) and (b) poly(HEA-*co*-NVP) polymers prepared by inhomogeneous biphase FP versus monomer weight ratios. Initial conditions: phase-1, DMSO = 50 wt%, MBAA = 0.3 wt%, APS = 0.2 wt%, [APS]/[TMEDA] = 1:4 (mol/mol); phase-2, glycerol = 50 wt%, MBAA = 0.25 wt%, APS = 0.2 wt%, [APS]/[TMEDA] = 1:4 (mol/mol).

3.4 FTIR and TGA characterizations of the dual-component poly(AM-*co*-NVP) and poly(HEA-*co*-NVP) polymers

FTIR characterizations were conducted to analyse the chemical composition of dual-component poly(AM-*co*-NVP) and poly(HEA-*co*-NVP) polymers fabricated by inhomogeneous biphase FP. The FT-IR spectrum of poly(AM-*co*-NVP) presents characteristic absorption peaks at 3430 cm^{-1} reflecting the stretching vibrations of –NH group of AM, and at 1298 cm^{-1} corresponding to the stretching vibration of C–N group of NVP, as indicated in Figure 5 (1). Figure 5 (2) demonstrates the FT-IR spectra of poly(HEA-*co*-NVP): a strong absorption peak at 3440 cm^{-1} can be assigned to the stretching vibration of –OH group of HEA and the absorption peak at 1295 cm^{-1} relates to the stretching vibration of C–N group of NVP. TGA thermograms of poly(AM-*co*-NVP) and poly(HEA-*co*-NVP) polymers in nitrogen environment with the temperature range from 200 to 800 °C are demonstrated in Figure 6a-b, respectively. The single degradation step in each TGA curves signifies that the as-prepared resultant hydrogels are single copolymer, further suggesting the successful synthesis of dual-component poly(AM-*co*-NVP) and poly(HEA-*co*-NVP) polymers.

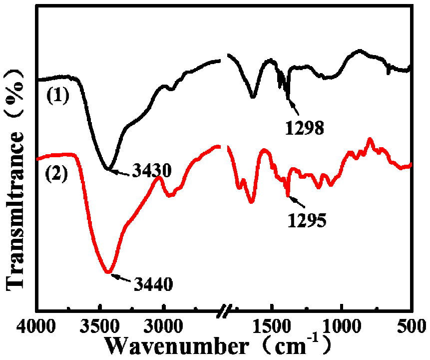

Fig. 5 FT-IR spectra of (1) poly(AM-*co*-NVP) and (2) poly(HEA-*co*-NVP).

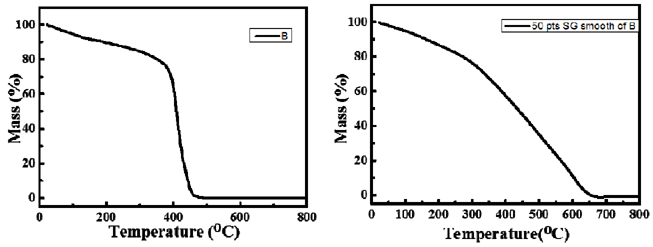

Fig. 6 TGA curves of (a) poly(AM-*co*-NVP) and (b) poly(HEA-*co*-NVP) polymers prepared by inhomogeneous biphase FP.

3.5 Morphologies of the dual-component poly(AM-*co*-NVP) and poly(HEA-*co*-NVP) polymers

The morphology of sample was analyzed by SEM measurements in order to investigate the surface structure of poly(AM-*co*-NVP) and poly(HEA-*co*-NVP) polymers synthesized by inhomogeneous biphase FP. As indicated in Figure 7a-b, both poly(AM-*co*-NVP) and poly(HEA-*co*-NVP) polymers exhibit compactly arranged microporous structure with a relatively uniform porous size distribution.

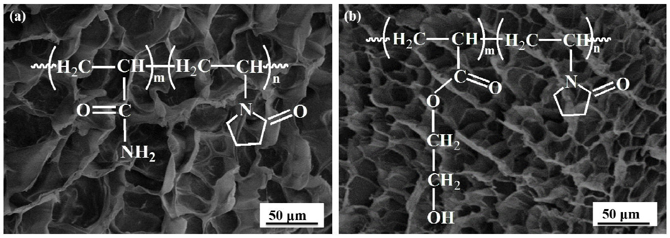

Fig 7 SEM micrographs of (a) poly(AM-*co*-NVP) and (b) poly(HEA-*co*-NVP) polymers. Initial conditions: phase-1, AM/NVP = 7:3 (wt/wt), DMSO = 50 wt%, MBAA = 0.3 wt%, APS = 0.2 wt%, [APS]/[TMEDA] = 1:4 (mol/mol); phase-2, HEA/NVP = 7:3 wt/wt, glycerol = 50 wt%, MBAA = 0.25 wt%, APS = 0.2 wt%, [APS]/[TMEDA] = 1:4 (mol/mol).

3.6 Swelling Capacity of the dual-component poly(AM-*co*-NVP) and poly(HEA-*co*-NVP) polymers

The water swelling kinetics behavior of poly(AM-*co*-NVP) and poly(HEA-*co*-NVP) polymers synthesized by inhomogeneous biphase FP at different AM/NVP and HEA/NVP weight ratios immersed in water was investigated using a gravimetric approach. As indicated in Figure 8a-b, the swelling ratios (SRs) of all the samples rise to some degree with the elevated swelling time and finally tend to a balanced value, which is defined as equilibrium swelling ratio (ESR). The ESRs of poly(AM-*co*-NVP) polymers are larger than that of poly(HEA-*co*-NVP) polymers at the same AM/NVP and HEA/NVP weight ratio, which are in agreement with the results of morphological characteristics.

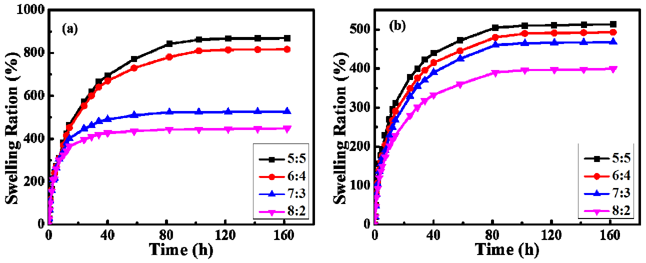

Fig. 8 Swelling kinetics of (a) poly(AM-*co*-NVP) and (b) poly(HEA-*co*-NVP) polymers with different AM/NVP and HEA/NVP weight ratios prepared by inhomogeneous biphase FP versus time. Initial conditions: phase-1, AM/NVP = 7:3 (wt/wt), DMSO = 50 wt%, MBAA = 0.3 wt%, APS = 0.2 wt%, [APS]/[TMEDA] = 1:4 (mol/mol); phase-2, HEA/NVP = 7:3 wt/wt, glycerol = 50 wt%, MBAA = 0.25 wt%, APS = 0.2 wt%, [APS]/[TMEDA] = 1:4 (mol/mol).

3.7 Horizontal inhomogeneous biphase FP of the dual-component bilayer film toward in-situ generation of white light-emitting fluorescent polymer nanocomposites

In order to obtain a dual-component bilayer films, inhomogeneous biphase FP in the horizontal direction was carried out. The appropriate amounts of phase-2 and phase-1 solutions were sequentially converted into a glass vessel, respectively (70 mm×15 mm) and then the mixture was horizontally triggered by laser at one end of the vessel. As shown in Figure 9a, we can clearly observe the propagating front moving at a constant velocity of ~14 mm/min, indicating pure FP has occurred.

By adding appropriate amount of CDs (molar concentration = 0.3 mM, λem= 471 nm) in phase-1 solution and CdTe QDs (mass concentration = 0.018 wt %, λem= 587 nm) in phase-2 solution, a bilayer films with dual fluorescent signals from CDs and CdTe QDs were constructed via horizontally directed inhomogeneous biphase FP. The PL spectra of the fluorescent bilayer film with emission wavelength spreading the visible range from 400 to 700 nm is shown in Figure 9b and Figure 9c presents the fluorescent image of the bilayer film emitting white light under a UV lamp (λ = 365 nm). White LEDs were then fabricated by applying the as-prepared fluorescent bilayer film onto a UV light-emitting diode (LED), in which semiconductor diodes were used to excite inorganic CDs, CdTe QDs and dual-component polymer, as demonstrated in Figure 9d. Commission Internationale de l'Eclairage (CIE) chromaticity coordinates of the white LED is (0.31, 0.28), which belongs to the white gamut, as shown in Figure 9e. The successful fabrication of white LED based on fluorescent bilayer film with two compensating colors is potentially useful in the white color optoelectronic devices.

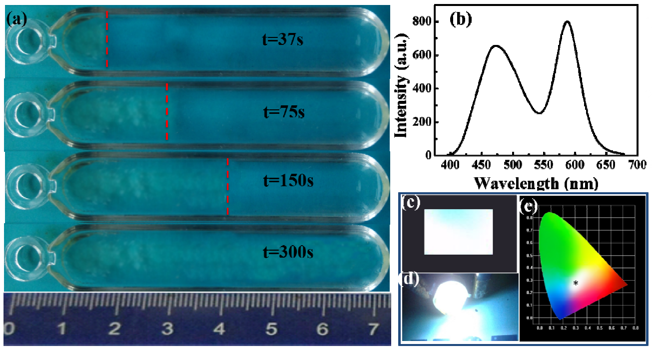

Fig. 9 (a) Photos of the propagating front of the horizontal inhomogeneous biphase FP. (b) PL emission spectra of fluorescent bilayer films. (c) Digital photograph of fluorescent bilayer films under UV light. (d) The emitted white light of the LED device in the dark. (e) CIE 1931 chromaticity diagram and the positions (marked by the asterisk) under UV irradiation (λ = 365 nm).

4. Conclusions

In summary, dual-component poly(AM-*co*-NVP) and poly(HEA-*co*-NVP) continuous polymers have been successfully prepared based on two immiscible phases via laser-ignited inhomogeneous biphase FP. The dependence of the frontal velocities and temperatures on initiator concentration and the monomer mass ratios have been thoroughly investigated. Perhaps more importantly, through the introduction of carbon dots (CDs) and quantum dots (QDs), an operable dual-component bilayer film with two fluorescent signals was fabricated via laser-ignited inhomogeneous biphase FP in the horizontal direction, toward in-situ generation of white light-emitting fluorescent polymer nanocomposites. Moreover, the white LED was fabricated by applying the as-prepared fluorescent bilayer film onto a UV LED, which used as an excitation source. The methodology developed in this work will open an alternative pathway to develop various inhomogeneous multicomponent polymers with combined functions towards optoelectronic devices.

Acknowledgements

This work was supported by National Natural Science Foundation of China (21006046 and 21474052), Natural Science Foundation of Jiangsu Province (BK20131408), Priority Academic Program Development of Jiangsu Higher Education Institutions (PAPD) and Jiangsu Overseas Research & Training Program for University Prominent Young & Middle-aged Teachers and Presidents.

Notes and references

State Key Laboratory of Materials-Oriented Chemical Engineering, and College of Chemistry and Chemical Engineering, Nanjing Tech University (former: Nanjing University of Technology), Nanjing 210009, P. R. China.
Corresponding author: Su Chen, Email: chensu@njtech.edu.cn

1 N. M. Chechilo, R. JKhvilivitskii and N. S. Enikolopyan, *Dokl. Akad. Nauk SSSR*, 1972, **204**, 1180-1181.
2 A. M. Khan and J. A. Pojman, *Trends Polym. Sci.*, 1996, **4**, 253-257.
3 J. A. Pojman, G. Curtis and V. M. Ilyashenko, *J. Am. Chem. Soc.*, 1996, **118**, 3783-3784.
4 P. M. Goldfeder, V. A. Volpert, V. M. Ilyashenko, A. M. Khan, J. A. Pojman and S. E. Solovyov, *J. Phys. Chem. B*, 1997, **101**, 3474-3482.
5 A. Mariani, S. Fiori, S. Bidali, V. Alzari and G. Malucell, *J. Polym. Sci. Part A: Polym. Chem.*, 2008, **46**, 3344-3352.
6 S. Fiori, A. Mariani, L. Ricco and S. Russo, *Macromolecules*, 2003, **36**, 2674-2679.
7 S. Chen, J. J. Sui, L. Chen and J. A. Pojman, *J. Polym. Sci. Part A: Polym. Chem.*, 2005, **43**, 1670-1680.
8 Y. A. Chekanov and J. A. Pojman, *J. Appl. Polym. Sci.*, 2000, **78**, 2398-2404.
9 J. Masere, L. L. Lewis and J. A. Pojman, *J. Appl. Polym. Sci.*, 2001, **80**, 686-691.

10 I. P. Nagy, L. Sike and J. A. Pojman, *Adv. Mater.*, 1995, **7**, 1038-&.

11 J. A. Pojman, W. Elcan, A. M. Khan and L. Mathias, *J. Polym. Sci. Part A: Polym. Chem.*, 1997, **35**, 227-230.

12 N. Liu, H. Shao, C. F. Wang, Q. L. Chen and S. Chen, *Colloid. Polym. Sci.*, 2013, **291**, 1871-1879.

13 Q. Feng, F. Li, Q. H. Yan, Y. H. Zhu and C. H. Ge, *Colloid. Polym. Sci.*, 2010, **288**, 915-921.

14 R. P. Washington and O. Steinbock, *J. Am. Chem. Soc.*, 2001, **123**, 7933-7934.

15 G. D. Lu, Q. Z. Yan and C. C. Ge, *Polym. Int.*, 2007, **56**, 1016-1020.

16 V. Alzari, O. Monticelli, D. Nuvoli, J. M. Kenny and A. Mariani, *Biomacromolecules*, 2009, **10**, 2672-2677.

17 Y. Fang, H. Yu, L. Chen and S. Chen, *Chem. Mater.*, 2009, **21**, 4711-4718.

18 J. Tu, L. Chen, Y. Fang, C. F. Wang and S. Chen, *J. Polym. Sci. Part A: Polym. Chem.*, 2010, **48**, 823-831.

19 V. Alzari, D. Nuvoli, S. Scognamillo, M. Piccinini, E. Gioffredi, G. Malucelli, S. Marceddu, M. Sechi, V. Sanna and A. Mariani, *J. Mater. Chem.*, 2011, **21**, 8727-8733.

20 S. Scognamillo, V. Alzari, D. Nuvoli, J. Illescas, S. Marceddu and A. Mariani, *J. Polym. Sci. Part A: Polym. Chem.*, 2011, **49**, 1228-1234.

21 R. B. Zhang, Z. X. Qiu, H. X. Qiu and X. H. Zhang, *J. Appl. Polym. Sci.*, 2014, **131**.

22 N. S. Pujari, A. R. Vishwakarma, T. S. Pathak, A. M. Kotha and S. Ponrathnam, *Bull. Mater. Sci.*, 2004, **27**, 529-535.

23 E. Gavini, A. Mariani, G. Rassu, S. Bidali, G. Spada, M. C. Bonferoni and P. Giunchedi, *Eur. Polym. J.*, 2009, **45**, 690-699.

24 J. V. Crivello, *Polymer*, 2005, **46**, 12109-12117.

25 C. Nason, T. Roper, C. Hoyle and J. A. Pojman, *Macromolecules*, 2005, **38**, 5506-5512.

26 J. V. Crivello, *J. Polym. Sci. Part A: Polym. Chem.*, 2007, **45**, 4331-4340.

27 Z. Jimenez, C. Bounds, C. E. Hoyle, A. B. Lowe, H. Zhou and J. A. Pojman, *J. Polym. Sci. Part A: Polym. Chem.*, 2007, **45**, 3009-3021.

28 L. L. Lewis, C. S. Debisschop, J. A. Pojman and V. A. Volpert, *J. Polym. Sci. Part A: Polym. Chem.*, 2005, **43**, 5774-5786.

29 J. Zhou, W. Q. Tang, C. F. Wang, L. Chen, Q. L. Chen and S. Chen, *J. Polym. Sci. Part A: Polym. Chem.*, 2012, **50**, 3736-3742.

30 H. Shao, C. F. Wang, S. Chen and C. Xu, *J. Polym. Sci. Part A: Polym. Chem.*, 2014, **52**, 912-920.

31 Z. F. Zhou, C. Yu, X. Q. Wang, W. Q. Tang, C. F. Wang and S. Chen, *J. Mater. Chem. A*, 2013, **1**, 7326-7331.

32 W. Q. Tang, L. H. Mao, Z. F. Zhou, C. F. Wang, Q. L. Chen and S. Chen, *Colloid. Polym. Sci.*, 2014, **292**, 2529-2537.

33 Y. Li, S. Y. Yang, C. F. Wang and S. Chen, *J. Polym. Sci. Part A: Polym. Chem.*, 2015, **53**, 2085-2093.

34 Y. Liu, C. F. Wang and S. Chen, *RSC Adv.*, 2015, **5**, 30514-30521.

35 C. Yu, C. F. Wang and S. Chen, *Adv. Funct. Mater.*, 2014, **24**, 1235-1242.

36 C. Yu, C. F. Wang and S. Chen, *J. Mater. Chem. A*, 2015, **3**, 17351-17358.

37 W. C. Zhang, S. Y. Yang, C. F. Wang and S. Chen, *Macromolecules*, 2015, **48**, 5543-5549.

38 A. Budkowski, A. Bernasik, E. Moons, M. Lekka, J. Zemla, J. Jaczewska, J. Haberko, J. Raczkowska, J. Rysz and K. Awsiuk, *Acta Phys. Pol. A*, 2009, **115**, 435-440.

39 J. Du and R. K. O'Reilly, *Chem. Soc. Rev.*, 2011, **40**, 2402-2416.

40 S. N. Yin, C. F. Wang, Z. Y. Yu, J. Wang, S. S. Liu and S. Chen, *Adv. Mater.*, 2011, **23**, 2915-2919.

41 X. Li, L. Zhou, Y. Wei, A. M. El-Toni, F. Zhang and D. Zhao, *J. Am. Chem. Soc.*, 2014, **136**, 15086-15092.

42 C. Ma, T. Li, Q. Zhao, X. Yang, J. Wu, Y. Luo and T. Xie, *Adv. Mater.*, 2014, **26**, 5665-5669.

In Situ Access to Fluorescent Dual-Component Polymers towards Optoelectronic Devices via Inhomogeneous Biphase Frontal Polymerization

Qing Li, Wan-chao Zhang, Cai-Feng Wang, and Su Chen*

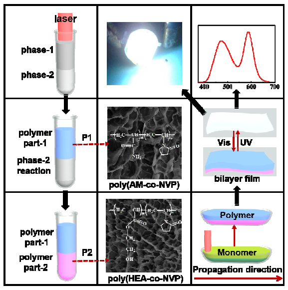

Fluorescent dual-component poly(AM-*co*-NVP) and poly(HEA-*co*-NVP) polymers used to generate white LEDs were in-situ synthesized via laser-ignited inhomogeneous biphase frontal polymerization.